IMPACT OF RECONFIGURABLE ANTENNAS ON INTERFERENCE ALIGNMENT

Rohit Bahl

A THESIS

in

Telecommunications and Networking

Presented to the Faculties of the University of Pennsylvania in Partial Fulfillment of the Requirements for the Degree of Master of Science in Engineering

2012

Supervisor of Thesis

Graduate Group Chairman

Contents

List of Figures **iv**

List of Tables **v**

1 Introduction **1**

1.1 Motivation 4

1.2 Contribution 6

1.3 Outline 7

1.4 Mathematical Notations 7

2 Background **8**

2.1 System Model 8

2.2 Interference Alignment 10

2.3 Blind Interference Alignment 16

2.4 Reconfigurable Antennas 21

3 Experimental Setup **23**

3.1 Enhanced Interference Alignment 23

3.2 Reconfigurable Antennas 27

3.2.1 Reconfigurable Circular Patch Array (RCPA) 27

3.2.2 Reconfigurable Printed Dipole Array (RPDA) 29

3.3 Measurement Setup 31

3.3.1 3 user 2×2 MIMO scenario 31

4 Results and Discussion **34**

4.1 Performance Metrics and Evaluation 35

4.1.1 Normalization of Channel Values 35

4.1.2 Ergodic Sum Capacity 37

4.1.3 Chordal Distance 41

4.1.4 Degrees of Freedom achieved 43

4.2 Results and Discussion 44

4.2.1 Closed form IA 44

5 Conclusion and Future Work **52**

5.1 Future Work 53

References **57**

List of Figures

1.1 Two user Gaussian Interference Channel 2

2.1 Conceptual representation of the three user 2×2 MIMO interference channel 10

2.2 Conceptual representation of Interference Alignment at user 1 11

2.3 Conceptual representation of antenna switching patterns for Blind Interference Alignment in 2 user 2×1 MISO network 18

2.4 Super symbol structure for 2 user 2×1 MISO network [1] 19

3.1 Conceptual representation of enhanced subspaces achieved using reconfigurable antennas 26

3.2 RCPA Radiation Patterns (in dB) in the azimuthal plane at Port 1 and 2. a) port 1: *Mode3*, port 2: *Mode3*; b) port 1: *Mode4*, port 2: *Mode4* 29

3.3 RPDA Radiation Patterns (in dB) in the azimuthal plane with antenna element separation of $\lambda/4$. a) *short-short*; b) *long-short*; c) *short-long*; d) *long-long* 30

3.4 3 User 2×2 MIMO Indoor Experimental Setup 32

4.1 Conceptual representation of transformation from Euclidean space to Grassmann Manifold 42

4.2 CDF of the total chordal distance achieved via RPDA 45

4.3 CDF of the total chordal distance achieved via RCPA 46

4.4 Empirical CDF plot of Sum - Capacity for RPDA (SNR = 20 dB) . 48

4.5 Empirical CDF plot of Sum - Capacity for RCPA (SNR = 20 dB) . . 49

4.6 Sum-Rate v/s SNR for RPDA 50

4.7 Sum-Rate v/s SNR for RCPA 50

List of Tables

1.1 Summary of basic techniques for mitigating interference in multi user networks 3

3.1 Spatial correlation between patterns generated at two different ports of RCPA 28

3.2 Spatial correlation between patterns generated at the same port of the RCPA 28

3.3 Measured Radiation efficiency of the RCPA 28

3.4 Spatial correlation between patterns generated at the same port of the RPDA 30

3.5 Spatial correlation between patterns generated at the same port of the RPDA 31

3.6 Measured Radiation efficiency of the RCPA 32

4.1 Mean value of total chordal distance 47

4.2 Comparison of mean value of sum capacity achieved 51

4.3 Degrees of Freedom (DoF) achieved 51

List of Notations

BC Broadcast Channel 39

BIA Blind Interference Alignment 16

CDF Cumulative Distribution Function 44

DoF Degrees of Freedom 4

IA Interference Alignment 3

IC Interference Channel 2

INR Interference to Noise Ratio 3

MAC Multiple Access Channel 39

MIMO Multiple Input Multiple Output 2

MISO Multiple Input Single Output 17

RA Reconfigurable Antennas 5

RCPA Reconfigurable Circular Patch Antennas 27

RPDA Reconfigurable Printed Dipole Arrays 29

SNR Signal to Noise Ratio 3

Abstract

Establishing the capacity regions of multiuser interference channels has been the holy grail of wireless communications ever since the pioneering work of C.E Shannon on the capacity of AWGN channels. Although considerable advancement has been made in our understanding of the interference channel, still the capacity regions remain unknown. For almost half a century it was believed that the Degrees of Freedom (DoF) of a K user interference channel did not scale with the number of transmitters in the network. In other words, wireless networks were thought to be limited by the amount of interference power each receiver experienced. Contrary to this popular notion, Cadambe and Jafar proved that concentrating interference and desired signal into separate spaces using Interference Alignment (IA) based precoding, could achieve the outer bound of the DoF for the interference channel. However, the non-orthogonality of signal and interference space limits sum-rate performance of interference alignment.

In this thesis, we consider the combination of reconfigurable antennas and interference alignment schemes to achieve enhanced sum rate performance via increased

subspace orthogonality. We present the notion that by using reconfigurable antenna based pattern diversity, optimal channel can be realized in order to maximize the distance between the interference and signal subspaces, thereby increasing sum-rate. We experimentally validate our claim and show the benefits of pattern reconfigurability using real-world channels, measured in a MIMO-OFDM interference network. We quantify the results with two different reconfigurable antenna architectures and show that substantial gains in chordal distance and sum capacity can be achieved by exploiting pattern diversity with IA. We further show that due to optimal channel selection, the performance of IA can also be improved in the low SNR regime, which is where interference alignment has been shown to be suboptimal.

Dedicated to my parents and sister.

Acknowledgements

First and foremost, I would like to extend my sincere gratitude towards Professor Dwight Jaggrad, whose unconditional support has made this work possible. I feel indebted to him, for it is because of the encouragement he provided throughout the program that finally led to the completion of this work. His suggestions on how academic research should be approached became my guiding principles during the times when I needed them the most. I feel deeply honored to have had this opportunity of working with him during my stay at the University of Pennsylvania.

I consider myself extremely fortunate to have had the guidance of Dr. Kapil Dandekar, who graciously agreed to be my co-advisor and was kind enough to offer collaboration with the Drexel Wireless Systems Lab. His guidance, subject matter expertise and enthusiasm towards the domain had a profound impact on my work. It is because of the faith he installed in me that I was able to pursue my interests and eventually bring them to a closure. I hope that this work is a starting chapter in a long lasting collaboration.

It is difficult for me to overstate the guidance I received from a fellow graduate student and a dear friend, Nikhil Gulati, whom I thank for introducing me to the domain of Interference Alignment, which eventually became the core of my research. All the technical discussions that we had became the building blocks for this work. It is hard for me to imagine this work without your support, motivation and inspiration.

Working in the Drexel Wireless Systems Lab brought me in contact with some of the most intellectual and wonderful people I have met during my academic career and deserve a word of thanks for inducting me in the research group as one of their own. I wish to thank David Gonzalez, for always being there to answer my questions on MIMO-OFDM and helping me throughout the experimental work. Kevin Wanuga, for the long sessions on analysis of the experimental data, and helping me understand the fine details of MIMO systems. And, I can't be more thankful to John Kountouriotis, who was kind enough to share his extensive and in depth experience in wireless systems.

Finally, I would like to thank and dedicate this thesis to my parents and sister, who have always rendered their unconditional love and support to me. Thank you for always being there to support me when I needed it the most.

Chapter 1

Introduction

Interference and fading are two central phenomena in wireless communications. Fading is a naturally occuring effect in which the information carrying radio frequency (RF) wave is attenuated by the channel of propagation, decreasing the power of desired signal. Interference on the other hand arrises when two or more trasmitters located in vicinity, start to contend for shared transmission resources such as time slots, frequency etc.

To understand the fundamental nature of wireless channels, C.E Shannon in 1948 developed a new branch of mathematics, *Information Theory*, which is used as the basic tool for analysis of these two central effects. While a lot of progress has been made since then in understanding and mitigating fading effects via spectrum efficient

techniques such *Multiple Input Multiple Output* (MIMO) and opportunistic communications, the same is not true for interference. For majority of the network architectures deployed today, such as cellular, ad-hoc and WLAN, interference still remains a limiting factor. This can be attributed to the fact that interference channel are not yet fully understood and their capacity largely remains unknown. The non-trivial nature of their analysis is exemplified by the fact that even the capacity region of the simplest of interference channel (IC), a two user gaussin interference channel (Fig. 1.1), has remained an open problem for more than 40 years now [2].

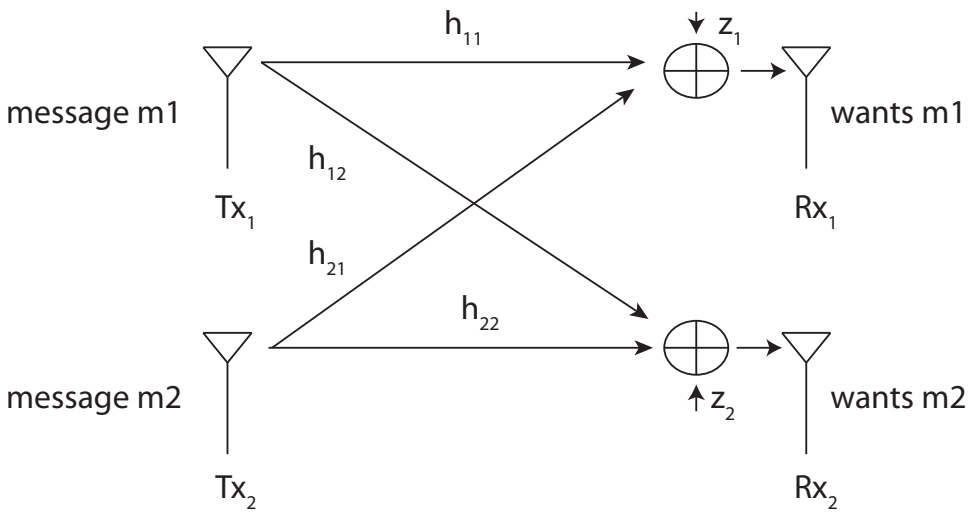

Figure 1.1: Two user Gaussian Interference Channel

Majority of the wireless networks deployed today, use one of the methods listed in Table 1.1 for managing interference, the most popular being orthogonalization of resources. It is well know that while orthogonalization of resources is relatively easily

achieved even for large network, its capacity asymptotically goes to zero, which limits its applicability for serving next generation of networking that aim to serve bandwidth hungry applications. For the two user interference channel shown in Fig. 1.1, when the Signal to Noise Ratio (SNR) at the receiving device is relatively larger than the Interference to Noise Ratio (INR), it has been shown in [3] that the optimal strategy for each receiver would be to decode the received interference, with the caveat that the all the messages must be public, i.e. decodable by the receivers in the network. When the messages are private though and SNR $\gg$ INR, treating the interference as noise has been shown to be optimal. These results, although insightful, are not easy to generalize for more than 2 users. Then to study the K user IC, we move towards the fourth interference management strategy, which has been recently proposed, Interference Alignment (IA) .

Table 1.1: Summary of basic techniques for mitigating interference in multi user networks

Orthogonalise the resources via TDMA/FDMA etc	Treat interference as gaussian Noise
Decode interference in SNR regions	Align all the interference vectors via interference alignment

1.1 Motivation

Interference management in multiuser wireless networks is a critical problem that needs to be addressed for enhancing network capacity. Cadambe and Jafar [4] made an important advancement in this direction by proving that the sum capacity of a multiuser network is not fundamentally limited by the amount of interference. In contrast with the traditional view, the number of interference free signaling dimensions, referred to as Degrees of Freedom (DoF), were shown to scale linearly with the number of users. Subsequently, they proposed Interference Alignment (IA) based precoding to achieve linear scaling of DoF and sum capacity in the high SNR regime.

The key insight for IA, is that perfect signal recovery is possible if interference does not span the entire received signal space. As a result, a smaller subspace free of interference can be found where desired signal can be projected while suppressing the interference to zero (Fig. 2.1). Since the component of the desired signal lying in the interference space is lost after projection, the sum-rate scaling achieved comes at the expense of reduced SNR [5]. Therefore, in order to achieve optimal performance, the two spaces must be roughly orthogonal. However, as the results in [6] show, orthogonality (represented in terms of chordal distance) of the subspaces is influenced by the nature of wireless channel and hence may not always be achievable in real world. Further, the authors provided a feasibility study of IA over measured channels and established an empirical relation between sum-rate and distance between the sig-

nal and interference space. They quantified the effect of correlated channels on the sum capacity and show the sub-optimality of IA at low SNR. Another experimental study reported in [7] showed similar degradation in the performance of IA because of practical effects such as collinearity of subspaces arising in real world channels. On the other hand, reconfigurable antennas have been shown to enhance the performance of MIMO systems by increasing the channel capacity, diversity order and even have been shown to perform well in the low SNR regimes [8], [9], [10]. The ability of reconfigurable antennas to dynamically alter the radiation patterns and provide multiple channel realizations enable MIMO systems to adapt according to physical link conditions which leads to improved capacity. In the context of IA, reconfigurable antennas have the potential to improve its sum-rate by providing potentially uncorrelated channel realizations.

In this work, we propose to exploit the pattern diversity offered by reconfigurable antennas to achieve an improved sub space design for IA. We experimentally evaluate the performance impact of pattern diversity on interference alignment over wideband MIMO interference channel, using three user 2×2 MIMO-OFDM channel data. The measurements were accomplished by employing two different architectures of reconfigurable antennas, which allow us to study the impact of antenna design and characteristics on the performance of IA. We provide analysis in terms of the improvements achieved in sum capacity, degrees of freedom and distance between interference

and desired signal space. Through our experimental results, we show that reconfigurable antennas offer additional capacity gains in combination with IA and provide a first step in motivating the use of these antennas for enhancing interference management techniques. To the best of our knowledge, previous experimental studies on quantifying the performance of IA, limit the antenna to be omnidirectional and no experimental study has been conducted for evaluating the performance of reconfigurable antennas in networks using IA for interference management.

1.2 Contribution

The first contribution of this thesis is the notion that the sum capacity of interference alignment precoding can be substantially increased by employing reconfigurable antennas instead of omnidirectional antennas. This enhanced sum rate performance is achieved by improving the orthogonality of the signal and interference sub spaces. We show that the gains achieved are more prominent in the low SNR region, which is the typical region for sub optimal performance of interference alignment. We experimentally validate our claim and present the benefits of pattern reconfigurability obtained in IA. We quantify the results with two different reconfigurable antenna architectures and show that substantial gains in chordal distance, which compares the two subspaces, are correlated with the enhanced sum capacity achieved via pattern reconfigurability.

1.3 Outline

Chapter 2 provides an introduction to the system model assumed for the rest of this thesis, concepts and algorithms of both blind and closed form interference alignment, and the theory of reconfigurable antennas. In Chapter 3, we present experimental setup used to collect data for analyzing closed form interference alignment, and the architectures of the reconfigurable antennas used in the measurement process. Discussion about the performance metrics used and the results obtained is presented in Chapter 4. Finally, we present the concluding remarks and the outline for prospective future work in Chapter 5.

1.4 Mathematical Notations

The following notations will be used throughout this paper. Capital bold letters ($\mathbf{H}$) shall denote matrices and small bold ($\mathbf{h}$) letters shall represent vectors. $\mathbf{H}^{-1}$, $\mathbf{H}^{\dagger}$ and $\mathbf{H}^{T}$ will be used to denote the matrix inverse, hermitian and transpose operation respectively. The space spanned by the columns of matrix $\mathbf{H}$, will be represented by span($\mathbf{H}$) whereas the null space of $\mathbf{H}$ will be represented by null($\mathbf{H}$). $\|\mathbf{H}\|_F$ will represent the Frobenius norm of the matrix $\mathbf{H}$. The d $\times$ d identity matrix will be represented by $\mathbf{I}_d$. $\mathbb{C}$ and $\mathbb{R}$ will represent the complex and real spaces respectively.

Chapter 2

Background

2.1 System Model

To study the impact of using reconfigurable antennas on IA, we restrict our analysis to the three user 2×2 MIMO-OFDM IC as depicted in Fig. 2.1. This ensured tractability of the analysis and in no respect represents any limitation on the applicability of reconfigurable antennas in other types of network setups.

Consider an ad-hoc interference network composed of K transmitters and K receivers, where the kth transmitter, $k \in \{1, 2, 3, ... \text{ K }\}$, intends to transmit a message $\mathbf{x}^k$, to the rth receiver. While every transmitter has a message for only one unique receiver, there exists a channel between all the pairs of transmitters and receivers,

represented by $\mathbf{H}^{[i,j]}$, creating a multiuser interference channel. Therefore, the message $\mathbf{x}^k$, k $\in \{1, 2, 3, ...K\}$, interferes with $K-1$ receivers. Each transmitter (Tx) in the network is equipped with M reconfigurable antennas and each receiver (Rx) is equipped with N reconfigurable antennas. The reconfigurable antennas at the transmitter and receiver have $\mathcal{P}$ and $\mathcal{Q}$ reconfigurable states respectively. Each of these states correspond to a unique radiation pattern. In such a setting, the received signal at the ith receiver can then be represented by

$$\mathbf{y}^{[i]}(f) = \mathbf{H}_{q,p}^{[i,i]}(f)\mathbf{x}^{[i]}(f) + \sum_{\substack{k=1 \\ k\neq i}}^{K} \mathbf{H}_{q,p}^{[i,k]}(f)\mathbf{x}^{[k]}(f) + \mathbf{n}^{[i]}(f), \tag{2.1.1}$$

where f denotes the OFDM subcarrier index and q, p represent the antenna state selected at the receiver and transmitter respectively, $\mathbf{y}$ is the $N \times 1$ received column vector, $\mathbf{H}_{q,p}^{[i,j]}$ is the $N \times M$ MIMO channel between Tx j and Rx i, $\mathbf{x}^{[k]}$ is the $M \times 1$ input column vector and $\mathbf{n}$ represents the $N \times 1$ vector of complex zero mean Gaussian noise with covariance matrix $\mathbb{E}\left[\mathbf{n}\mathbf{n}^{\dagger}\right] = \sigma^2 \mathbf{I}_N$. The total number of data carrying OFDM subcarriers will be represented by F_s ($F_s = 52$). For brevity, we will drop the symbols f, p and q. Here $\mathbf{x} \in \mathbb{C}^{M\times 1}$, $\mathbf{y} \in \mathbb{C}^{N\times 1}$ and $\mathbf{H} \in \mathbb{C}^{N\times M}$. The input vector $\mathbf{x}$ is subject to an average power constraint, $\mathbb{E}\left[Tr(\mathbf{x}\mathbf{x}^{\dagger})\right] = P$. Total power is assumed to be equally distributed across the input streams, i.e. the input covariance matrix $\mathbf{Q} = \frac{P}{d_k}\mathbf{I}_{d_k}$, where d_k streams are transmitted by the kth transmitter. Throughout this paper, we will restrict our study to $K = 3$; $M = N = 2$ and $d_k = 1$, $\forall\ k \in \{1, 2, 3\}$. The space of all the links in the network for all the states of reconfigurable

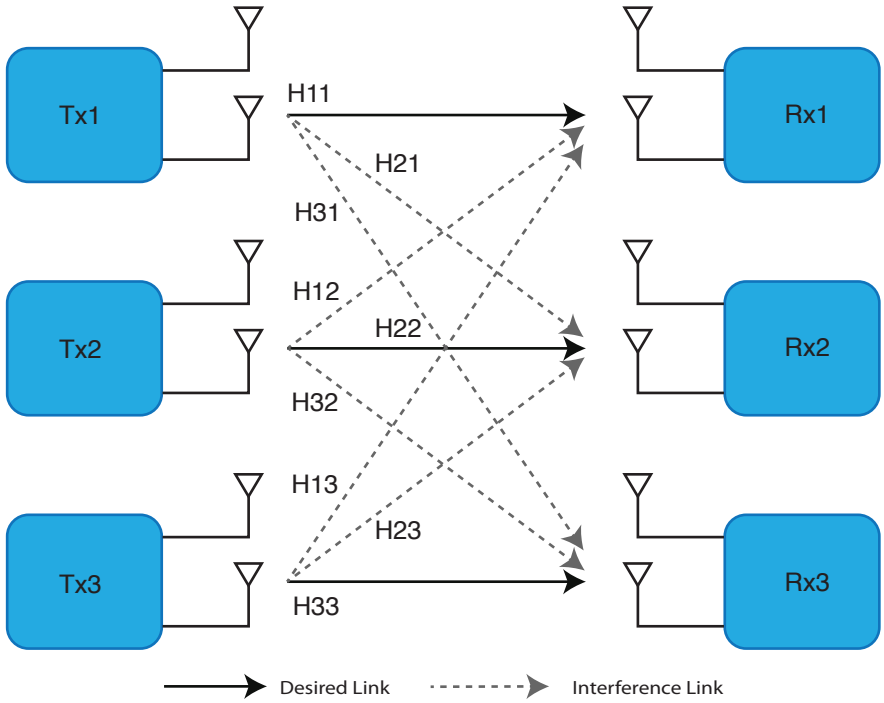

Figure 2.1: Conceptual representation of the three user 2×2 MIMO interference channel

antenna will be represented by the vector $\Omega = \{i_p, j_q\}$, $i, j \in \{1, 2, 3\}$, $p \in \mathcal{P}$ and $q \in \mathcal{Q}$.

2.2 Interference Alignment

Interference Alignment (IA) is a novel approach for mitigating interference in wireless networks that has recently emerged out of the seminal work in [4]. While the exact capacity regions of the interference channel remain unknown, approximate analysis

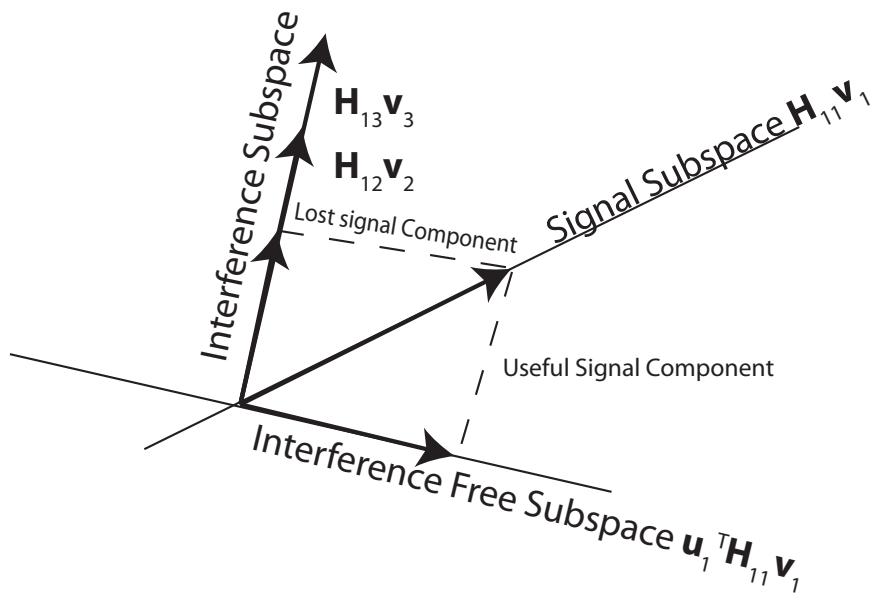

Figure 2.2: Conceptual representation of Interference Alignment at user 1

of the system through *degrees of freedom*, has given powerful insights into channel characteristics. The most striking result to come out of [4] in this direction is that even in the presence of strong interference power, using IA, $\frac{K}{2}$ DoF can be achieved per user instead of the conventionally thought $\frac{1}{K}$ (K being the number of users in the network).

Interference Alignment achieves this linear scaling of sum-capacity by precoding the signal vectors at each transmitter such that they cast overlapping shadows at the receiver. The precoders force the interference and signal vectors at each receiver, to decompose into orthogonal sub-spaces of the received signal space. This alignment of signals can be achieved in frequency, space or time. We will limit our discussion of

IA to alignment in the spatial domain.

To motivate the concept of IA, let us consider a system of underdetermined linear equations [11], i.e. a system with more unknown variables than observable outcomes

$$\begin{aligned} y_1 &= h_{11}x_1 + h_{12}x_2.... + h_{1N}x_N \\ &\vdots \\ &\vdots \\ y_M &= h_{M1}x_1 + h_{M2}x_2.... + h_{MN}x_N \end{aligned} \tag{2.2.1}$$

where N > M. Equation 2.2.1 can be interpreted as a network with N transmitters, each equipped with single antenna, and a receiver equipped with M antennas. Further, let us assume that the receiver is interested in receiving messages from only a subset of transmitters, say x_i , $i \in \{1, 2...K\}$. However, since the receiver has fewer number of antennas than the number of transmitters in the network, it can not reliably decode its desired signal. This system then models an interference channel. For this system, we ask the following question, how can the receiver reliably decode its desired messages from the interference signal ? To answer this question, we represent (2.2.1) in its corresponding matrix notation

$$\mathbf{y}_{M\times 1} = \left[\mathbf{h}^1_{M\times 1}\mathbf{h}^2_{M\times 1}...\mathbf{h}^N_{M\times 1}\right]\mathbf{x}_{N\times 1} \tag{2.2.2}$$

and note that the N column vectors of dimensionality M, completely span the M dimensions. For the receiver to resolve its desired K signals, the corresponding columns

vectors, represented by $\mathbf{h}^k_{1\times M}$ must be in a space not spanned by the undesired vectors i.e.

$$\mathbf{h}^k_{M\times 1} \notin \text{span}\left(\mathbf{h}^i_{M\times 1}, i \in \{K+1..N\}\right) \tag{2.2.3}$$

Since, the undesired $K-N$ vectors completely span the available M dimension, (2.2.3) is not feasible. However, if we can restrict all the undesired $K-N$ signals to smaller than M dimensions, (2.2.3) will be feasible and desired messages could be recovered. This concept of keeping the undesired signal vectors concentrated in a smaller space is central to Interference Alignment.

In a network setting, the goal of IA is then to make the signal to interference ratio (SIR) infinite at the output of each receiver. Specifically, if each transmitter transmits D independent streams of information, then to achieve perfect alignment at each receiver, dimensionality of the interference space must be restricted to $N-D$ in a $\mathbb{C}^N$ dimensional received signal space [11]. That is, there is a D dimensional subspace in $\mathbb{C}^N$ which is free of interference. The design of the precoding filters for the MIMO interference channel forces interference to exist in a smaller subspace. It has been shown that designing such precoding filters is NP hard for the general MIMO system [12] and closed form solutions can only be found for certain special cases, e.g. three user 2×2 MIMO channel [4]. We discuss such a closed form solution for the 3 user 2×2 MIMO channel next.

Let $\mathbf{v}^{[i]}$ and $\mathbf{u}^{[i]}$ represent the transmit precoder and receive interference suppres-

sion filter respectively, where $i \in \{1, 2, 3\}$ and $\mathbf{v}^{[i]}$, $\mathbf{u}^{[i]} \in \mathbb{C}^{2\times 1}$. Moreover, $\mathbf{v}^{[i]}$ and $\mathbf{u}^{[i]}$ should satisfy the feasibility conditions for IA [13] given by

$$\mathbf{u}^{[k]\dagger}\mathbf{H}^{[kj]}\mathbf{v}^{[j]} = 0, \forall j \neq k, \tag{2.2.4}$$

$$\text{rank}\left(\mathbf{u}^{[k]\dagger}\mathbf{H}^{[kk]}\mathbf{v}^{[k]}\right) = 1. \tag{2.2.5}$$

Equation 2.2.4 and 2.2.5 imply that interference is aligned in the null($\mathbf{u}^{[k]}$) and the desired signal is received via a equivalent SISO channel. Although, enhanced sum-capacity can be achieved by using non-unitary precoders, but we will concentrate on the gains achived solely via IA and hence avoid adding any additional power in the input symbols i.e. we restrict $\mathbf{v}^{[i]}$ and $\mathbf{u}^{[i]}$ to be unitary, i.e. $\left\|\mathbf{v}^{[i]}\right\|_F, \left\|\mathbf{u}^{[i]}\right\|_F = 1$.

After precoding the input symbol $x^{[i]}$ with $\mathbf{v}^{[i]}$, the signal received at the ith receiver can be represented by (2.2.6). For perfect alignment at the ith receiver, the interference signal vectors represented by $\mathbf{H}^{[i,k]}\mathbf{v}^{[k]}$, $k \neq i$ in (2.2.6) must span a common subspace of the received signal space. For the system model under consideration, this alignment condition must be satisfied at each receiver, forming a chain of conditions i.e. the interference vectors from transmitter 2 and 3 need to be aligned at receiver 1, interference from transmitters 3 and 1 need to be aligned at receiver 1 and interference from 1 and 2 needs to be aligned at receiver 3. We can express these

alignment condition using the defined interference vectors as (2.2.7-2.2.9).

$$\mathbf{y}^{[i]} = \mathbf{H}^{[i,i]}\mathbf{v}^{[i]}x^{[i]} + \sum_{\substack{k=1\\k\neq i}}^{K} \mathbf{H}^{[i,k]}\mathbf{v}^{[k]}x^{[k]} + \mathbf{n} \tag{2.2.6}$$

$$\text{span}(\mathbf{H}^{[1,2]}\mathbf{v}^{[2]}) = \text{span}(\mathbf{H}^{[1,3]}\mathbf{v}^{[3]}) \tag{2.2.7}$$

$$\mathbf{H}^{[2,1]}\mathbf{v}^{[1]} = \mathbf{H}^{[2,3]}\mathbf{v}^{[3]} \tag{2.2.8}$$

$$\mathbf{H}^{[3,1]}\mathbf{v}^{[1]} = \mathbf{H}^{[3,2]}\mathbf{v}^{[2]} \tag{2.2.9}$$

Closed form solution for the alignment condition expressed in (2.2.7-2.2.9), given the feasibility constraints (2.2.4) and (2.2.5), can then be found by solving the following eigenvalue problem in $\mathbf{v}^{[i]}$

$$\text{span}(\mathbf{v}^{[1]}) = \text{span}(\mathbf{E}\mathbf{v}^{[1]}) \tag{2.2.10}$$

$$\mathbf{v}^{[2]} = \mathbf{F}\mathbf{v}^{[1]} \tag{2.2.11}$$

$$\mathbf{v}^{[3]} = \mathbf{G}\mathbf{v}^{[1]} \tag{2.2.12}$$

$$\mathbf{E} = \left(\mathbf{H}^{[3,1]}\right)^{-1}\mathbf{H}^{[3,2]}\left(\mathbf{H}^{[1,2]}\right)^{-1}\mathbf{H}^{[1,3]}\left(\mathbf{H}^{[2,3]}\right)^{-1}\mathbf{H}^{[2,1]} \tag{2.2.13}$$

$$\mathbf{F} = \left(\mathbf{H}^{[3,2]}\right)^{-1}\mathbf{H}^{[3,1]} \tag{2.2.14}$$

$$\mathbf{G} = \left(\mathbf{H}^{[2,3]}\right)^{-1}\mathbf{H}^{[2,1]} \tag{2.2.15}$$

$$\mathbf{v}^{[1]} = \text{Eigenvec}(\mathbf{E}). \tag{2.2.16}$$

where the function Eigenvec(), returns the eigenvectors of the matrix $\mathbf{E}$. Since, there can be one than one unique eigenvectors for the matrix $\mathbf{E}$, the alignment precoders are not unique. The ith receiver can then suppress all the interference

by projecting the received signal (2.2.6) on the orthogonal complement of the interference space (2.2.17) i.e., the interference suppression filter is given by $\mathbf{u}^{[i]} = \text{null}([\mathbf{H}^{[i,j]}\mathbf{v}^{[j]}]^T)$.

$$\mathbf{u}^{[i]\dagger}\mathbf{y}^{[i]} = \mathbf{u}^{[i]\dagger}\mathbf{H}^{[i,i]}\mathbf{v}^{[i]}x^{[i]} + \sum_{\substack{k=1\\k\neq i}}^{K}\mathbf{u}^{[i]\dagger}\mathbf{H}^{[i,k]}\mathbf{v}^{[k]}x^{[k]} + \mathbf{u}^{[i]\dagger}\mathbf{n} \tag{2.2.17}$$

$$= \mathbf{u}^{[i]\dagger}\mathbf{H}^{[i,i]}\mathbf{v}^{[i]}\mathbf{x}^{[i]} + \mathbf{u}^{[i]\dagger}\mathbf{n} \tag{2.2.18}$$

Note that $\mathbf{u}^{[i]\dagger}\mathbf{H}^{[i,i]}\mathbf{v}^{[i]}$ acts as the effective SISO channel between Tx/Rx pair (i, i).

2.3 Blind Interference Alignment

The closed form solution of interference alignment for a three user 2×2 MIMO network discussed in Sec. 2.2, achieves outer bound of the DoF for the interference channel. However, the caveat to this is the requirement of global and instantaneous channel knowledge at all the transmitters. This requirement is almost never satisfied in real world networks, which motivates the need for alignment schemes with lower overhead requirements. In [14], it was shown that even without the knowledge of instantaneous channel coefficients, under certain heterogeneous block fading models, alignment is not only possible, but can also achieve outer bound of DoF.

The key insight provided in [14] for *Blind Interference Alignment* (BIA) is that the knowledge of channel coherence intervals associated with different users can alone provide enough information for alignment. But the alignment scheme presented

in [14], [15] relied heavily on the assumption of block fading structure of the wireless channel. Since, wireless channels are stochastic in nature, such fading scenarios may or may not occur. In [1], it was proposed that this type of block fading can be realized by employing *reconfigurable antennas*. It was shown that only with the knowledge of switching patterns of the reconfigurable antennas, signals could be aligned.

To exemplify the algorithm first presented in [1], let us consider a 2×1 *Multiple Input Single Output* (MISO) network with 1 transmitter and 2 receivers. Both the receivers are equipped with pattern reconfigurable antennas, which are capable of dynamically switching their states to realize new channel structures. The transmitter is equipped with two omnidirectional antennas and wishes to transmit independently encoded messages $\mathbf{x}_1$ and $\mathbf{x}_2$, $\mathbf{x}_i \in \mathbb{C}^{1\times 2}$, to the receivers Rx1 and Rx2 respectively with maximum rate. The receivers switch the states of the reconfigurable antennas according to a predetermined pattern known to the transmitter, say pattern P_i, $i \in \{1, 2\}$. Other than this information, the transmitter has no CSI for the purpose of alignment. Note that the receivers might even be statistically indistinguishable to the transmitter without having any effect on alignment. Also, CSIR might still be required for zero forcing the received streams, but is not a requirement for alignment. Using this system model, we can express the signal received at the ith receive in any given time slot t as,

$$y_t^{[i]}(k) = \sum_{i=1}^{2} \mathbf{x}_t^{[i]} \mathbf{h}_t^{[i]}(k_i) + n_t^{[i]}, \tag{2.3.1}$$

where the index k represents the current state of the reconfigurable antenna, $n_t^{[i]}$ represents the additive white Gaussian noise with zero mean and unit variance and $\mathbf{h}$ represents the 2×1 MISO channel between the transmitter and i^{th} receiver. During

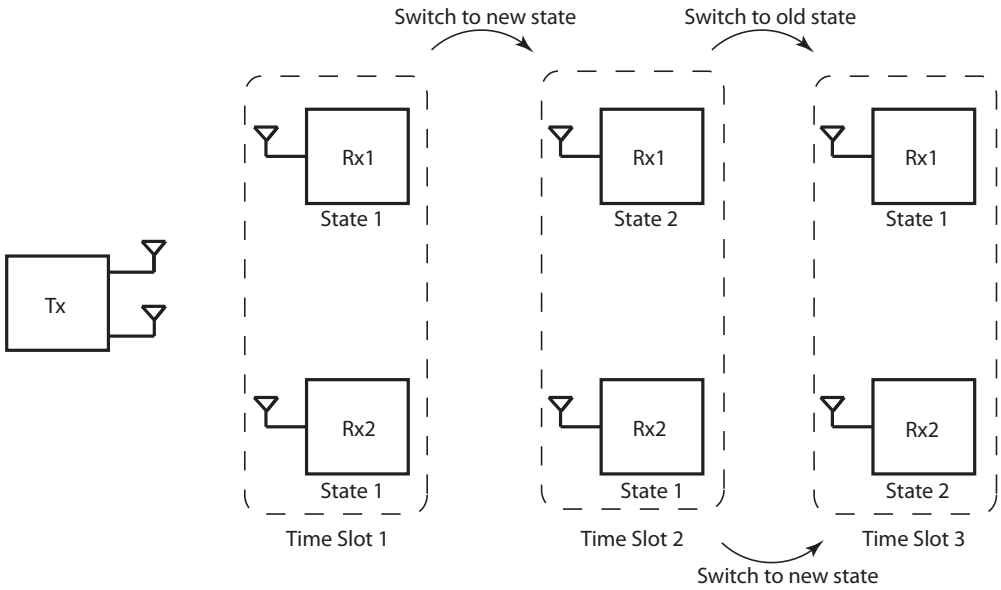

Figure 2.3: Conceptual representation of antenna switching patterns for Blind Interference Alignment in 2 user 2×1 MISO network

the transmission phase, the transmitter sends messages for both the receivers simultaneous. Message $\mathbf{x}_1$ then interferes with desired signal $\mathbf{x}_2$ at receiver two and vice versa. Using alignment we would be able to keep the signal and interference space orthogonal and hence minimize any interference. The key then to achieving blind alignment is the supersymbol structure depicted in Fig. 2.4. A supersymbol consists of the finite extensions in time required to achieve alignment. During the first time

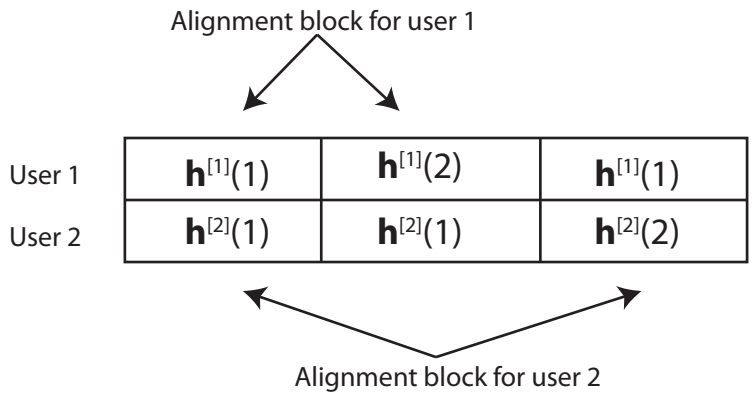

Figure 2.4: Super symbol structure for 2 user 2×1 MISO network [1]

slot of the supersymbol, the transmitter sends data for both the receivers, Rx1 and Rx2. In the second time slot, as depicted in the supersymbol structure, Rx1 switches to a new antenna state while Rx2 retains its state (Fig. 2.4). This creates an artificial fluctuation in the channel between the Tx and Rx1, keeping the channel between Tx and Rx2 unchanged. In this time slot, transmitter communicates data symbols for only Rx1, which is also received at Rx2. In the last slot of transmission, Rx1 switches back to its original configuration while Rx2 now makes a transition to a new state. Correspondingly, the transmitter now sends data symbols for only Rx2. This data transmission is described in terms of the beamforming matrices for the data of Rx1 and Rx2 in (2.3.2). The net signal vector received by Rx1 at the end of the first

supersymbol can then be represented as (2.3.3)

$$I_1 = \begin{bmatrix} \mathbf{I}_{2\times 2} \\ \mathbf{I}_{2\times 2} \\ \mathbf{0}_{2\times 2} \end{bmatrix}, I_2 = \begin{bmatrix} \mathbf{I}_{2\times 2} \\ \mathbf{0}_{2\times 2} \\ \mathbf{I}_{2\times 2} \end{bmatrix} \tag{2.3.2}$$

$$\begin{aligned} \begin{bmatrix} y_1^{[1]}(1) \\ y_2^{[1]}(2) \\ y_3^{[1]}(1) \end{bmatrix} &= \begin{bmatrix} h_1^{[1,1]}(1) & h_1^{[1,2]}(1) \\ h_2^{[1,1]}(2) & h_2^{[1,2]}(2) \\ h_3^{[1,1]}(1) & h_3^{[1,2]}(1) \end{bmatrix} \begin{bmatrix} \mathbf{I}_{2\times 2} \\ \mathbf{I}_{2\times 2} \\ \mathbf{0}_{2\times 2} \end{bmatrix} \begin{bmatrix} u_1^{[1]} \\ u_{[2]}^{1} \end{bmatrix} \\ &+ \begin{bmatrix} h_1^{[2,1]}(1) & h_1^{[2,2]}(1) \\ h_2^{[2,1]}(1) & h_2^{[2,2]}(1) \\ h_3^{[2,1]}(2) & h_3^{[2,2]}(2) \end{bmatrix} \begin{bmatrix} \mathbf{I}_{2\times 2} \\ \mathbf{0}_{2\times 2} \\ \mathbf{I}_{2\times 2} \end{bmatrix} \begin{bmatrix} u_1^{[2]} \\ u_2^{[2]} \end{bmatrix} + \begin{bmatrix} n_1^{[1]} \\ n_2^{[1]} \\ n_3^{[1]} \end{bmatrix} \end{aligned} \tag{2.3.3}$$

where $u_i^{[j]}$ represents an independent data symbol intended for receiver i transmitted from j^{th} antenna element. It should be noted here that the desired signal is received via a rank-2 matrix where as interference has been restricted to a rank-1 matrix. This permits the ith receiver to completely suppress the interference by a simple zero forcing filter:

$$\begin{bmatrix} y_1^{[1]}(1) - y_3^{[1]}(1) \\ y_2^{[1]}(2) \end{bmatrix} = \begin{bmatrix} h_1^{[1,1]}(1) & h_1^{[1,2]}(1) \\ h_2^{[1,1]}(2) & h_2^{[1,2]}(2) \end{bmatrix} \begin{bmatrix} u_1^{[1]} \\ u_2^{[1]} \end{bmatrix} + \begin{bmatrix} n_1^{[1]} - n_3^{[1]} \\ n_2^{[1]} \end{bmatrix}. \tag{2.3.4}$$

From (2.3.4), we note that, while the two independent messages,$u_1^{[1]}$ and $u_2^{[1]}$, intended for receiver 1 have been recovered after zero forcing, interference from the

symbols intended for receiver 2 has been completely eliminated. A similar zero forcing filter at the receiver 2 recovers the symbols $u_1^{[1]}$ and $u_2^{[2]}$, while completely eliminating interference from receiver 1. Since, we only used 3 time slots to transmit 4 independent messages, the DoF of the channel is $\frac{4}{3}$, whereas a simple TDMA approach could have only achieved a maximum of 1. In general, the DoF of a K user, M×1 MISO channel is given by

$$DoF_{K-MMISO} = \frac{MK}{M+K+1}. \tag{2.3.5}$$

2.4 Reconfigurable Antennas

Reconfigurable antennas are capable of changing the fundamental operating characteristics of the radiating elements either through electrical, mechanical or other means. Over that last ten years, research is primarily focused on designing reconfigurable antennas with the ability to dynamically change either frequency, radiation pattern and polarization or the combination of one of these properties [16]. These are essentially different than traditional phased array systems where phasing of signals between the array elements is used to achieve beamforming and beamsteering because the basic operating characteristics remain unchanged.

Antenna reconfigurability is sought for improving performance of communication links by dynamically adapting the antenna to changing operating environments. Besides the design challenges, the development of these antennas pose a significant

challenge challenge to system designers to integrate the reconfigurable antennas in existing wireless devices and networks. For the rest of the manuscript, we will only focus on pattern reconfigurable antennas and the pattern diversity offered by them.

Pattern reconfigurable antennas provide the ability to the change the shape or direction of the radiation pattern dynamically. In principle, the change in the arrangement of either electric or magnetic current through the antenna structure, effects the spatial distribution of radiation from the antenna element. This relationship makes the pattern reconfigurability possible [16]. Once the desired characteristics such as operating frequency is decided, there are various ways through which current distribution can be changed. These may include mechanical/structural changes, material variations, using electronic components like PIN diodes to change the dimensions of the antenna and so on.

Besides addressing the challenges in antenna architectures, it is essentially to quantify the performance of pattern reconfigurable antenna systems in communication systems. In recent years, many research groups have shown that reconfigurable antennas can offer additional performance gains in Multiple Input Multiple Output (MIMO) systems [17, 18, 19, 20, 21, 8] by increasing the channel capacity, diversity order and even have been shown to perform well in the low SNR regimes.

Chapter 3

Experimental Setup

3.1 Enhanced Interference Alignment

As discussed in Sec. 2.2, the criterion for design of IA precoding and decoding filters is minimization of interference. If perfect and instantaneous channel state information is available at all the transmitters in the network, IA precoders force interference vector to live in the same subspace. Consequently, interference power at each receiver terminal goes to zero or SIR is maximized. However, since IA only maximizes SIR, maximization of sum-capacity, the metric which we originally aimed to optimize, is not guaranteed. To exemplify this, let us consider the SINR and the SNR at the ith receiver denoted by $SINR^{i}_{no-IA}$ and SNR^{i}_{no-IA} respectively

$$SNR^i_{no-IA} = \frac{P_i \left\| \mathbf{H}^{[i,i]} \right\|_F}{\sigma^2}, \; SINR^i_{no-IA} = \frac{P_i \left\| \mathbf{H}^{[i,i]} \right\|_F}{\sigma^2 + \underbrace{\sum_{\substack{j=1 \\ j \neq k}}^{K} P_j \left\| \mathbf{H}^{[i,j]} \right\|_F}_{interference\ power}}. \tag{3.1.1}$$

Using the IA filters, $\mathbf{V}^{[i]}$, designed by the closed form algorithm discussed in Sec. 2.2, the $SINR_i$ can be written as

$$SINR^i = \frac{P_i \left\| \mathbf{H}^{[i,i]} \mathbf{V}^{[i]} \right\|_F^2}{\sigma^2 + \underbrace{\sum_{\substack{j=1 \\ j \neq i}}^{K} P_j \left\| \mathbf{H}^{[i,j]} \mathbf{V}^{[j]} \right\|_F^2}_{interference\ power}}. \tag{3.1.2}$$

Assuming perfect instantaneous CSI, zero forcing at the ith receiver completely removes all the interference power and the SNR_i and $SINR_i$ are reduced to

$$SNR^i_{IA} = \frac{P_i \left\| \mathbf{U}^{[i]\dagger} \mathbf{H}^{[i,i]} \mathbf{V}^{[i]} \right\|_F^2}{\sigma^2}. \tag{3.1.3}$$

It should be noted that since $\mathbf{U}^{[i]\dagger}\mathbf{H}^{[i,i]}\mathbf{V}^{[i]}$ represents the projection space of the original beam direction, $\mathbf{H}^{[i,i]}$, $SNR^i_{no-IA} > SINR^i_{IA}$. Moreover, the loss in signal power due to the component of desired signal lying in the interference space after projection, is high in the low SNR region. This decrease in SNR from optimal value reduces the capacity achieved by the network.

As noted from (3.1.3), the SNR achieved after IA depends upon the structure of the MIMO channel between the transmitter receiver pair, which in turn is determined by

the physical propagation environment. Although it is well known that SNR depends upon the strength of the eigenmodes of channel matrix $\mathbf{H}$, but in the context of IA, the channel structure additionally determines vector spaces optimal for transmission (Sec. 2.2). Suboptimal channels then may lead to poor design of transmit directions giving suboptimal capacity. Traditional omnidirectional antennas cannot change the physical propagation environment adaptive thereby admitting a loss in performance. In contrast, by dynamically changing their radiation patterns, reconfigurable antennas provide multiple channel realizations, which depending on the antenna architecture may be highly uncorrelated with each other. Using the new channel realizations, we design multiple beam directions, providing an additional degree of freedom for optimization. For selecting the most optimal state of transmission out of all the combinations in the network, we choose *chordal distance* (details in Sec. 4.1.3) as the preferred metric since it directly relates to channel states and capacity. The problem of optimal state selection then reduces to selecting the combination of states, which maximize the total chordal distance achieved. The effect of choosing the optimal states is conceptually demonstrated in Fig. 3.1.

Let us consider the three user 2×2 interference channel introduced in Sec 2.1, which uses IA as the preferred interference management strategy. In such network settings, the performances of all the links in the network are coupled to each other. A change in the transmit power by one transmitter, may lead to higher interference

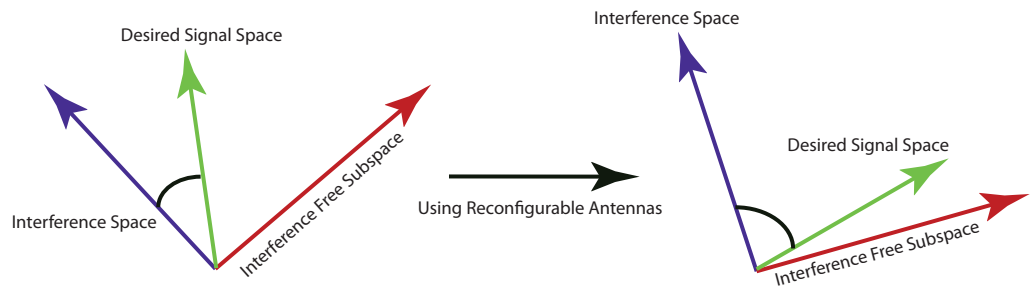

Figure 3.1: Conceptual representation of enhanced subspaces achieved using reconfigurable antennas

power in other links, which makes their analysis difficult. In the context of reconfigurable antennas, a change in the beam pattern of one of the transmitter/receiver will change the interference power seen at the other links. Therefore, to realize optimal capacity, we carry out joint optimization across all the link in the network. We use a centralized controller, which has instantaneous knowledge of global CSI to carry out this joint optimization and provide a loose upper bound on the performance of reconfigurable antennas in interference management. At each time slot t, the central controller calculates and selects the optimal precoders and zero forcing filters for all possible beam directions and sends feedback to the receiver/transmitter nodes. Since, as the number of possible configurations in the system increases, it becomes more challenging to select the optimal channel realization, we consider three different network configurations, where reconfigurable antennas are only at transmitter, only at receiver and both at transmitter and receiver. When employed at only one side

in the network, we will still consider reconfigurable antennas on the other side, but with fixed state that exhibits highest efficiency. These configurations then help us in reducing the search space for optimization and gives insights into the benefits of pattern diversity in downlink and uplink scenarios.

Next, we discuss the reconfigurable antennas used in our analysis, the differences in their relative performance and the experimental setup used to collect real world channel samples to design IA filters.

3.2 Reconfigurable Antennas

3.2.1 Reconfigurable Circular Patch Array (RCPA)

Reconfigurable Circular Patch Antennas (RCPA) [22] are capable of dynamically changing the shape of their radiation patterns by varying the radius of a circular patch. Each antenna has two feed points and can work as a two element array in a single physical device. By simultaneously turning the switches on or off, the RCPA can generate orthogonal radiation patterns at the two ports. This provides a total of two states of operation (Mode3 and Mode4) providing two unique radiation patterns. Also, the two antenna ports are fed such that the isolation between the two ports is higher than 20 dB. The measured radiation patterns in the azimuthal plane at the two ports of RCPA are shown in Fig. 3.2. [23]. Table 3.1 presents

the correlation between the patterns obtained from different ports, which as observed from the radiation patters also, is quite low. This helps in realizing channel samples which are highly uncorrelated. The downside of using RCPA is its poor radiation efficiency (Table 3.3), which leads to low SNR values at the receive antenna.

Table 3.1: Spatial correlation between patterns generated at two different ports of RCPA

Mode3	*Mode4*
.06	.18

Table 3.2: Spatial correlation between patterns generated at the same port of the RCPA

	$E_{1,mode3}$	$E_{1,mode4}$
$E_{1,mode3}$	1	0.2
$E_{1,mode4}$	0.2	1

Table 3.3: Measured Radiation efficiency of the RCPA

	Port 1(%)	*Port 2 (%)*
Mode 3	21	17
Mode 4	6	5

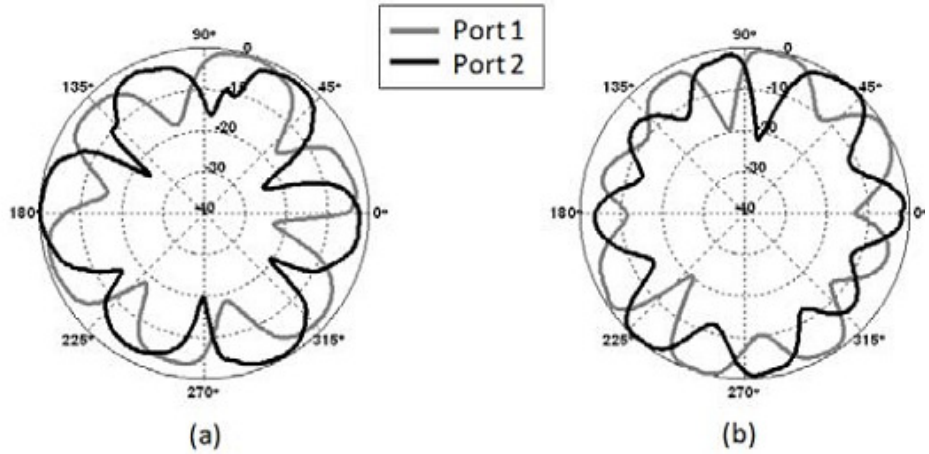

Figure 3.2: RCPA Radiation Patterns (in dB) in the azimuthal plane at Port 1 and 2. a) port 1: *Mode3*, port 2: *Mode3*; b) port 1: *Mode4*, port 2: *Mode4*

3.2.2 Reconfigurable Printed Dipole Array (RPDA)

A second type of pattern reconfigurable antenna used in our experiments is the Reconfigurable Printed Dipole Arrays (RPDA) [20]. In the array configuration, RPDAs are capable of generating multiple radiation patterns by electronically changing the length of the dipole. The multiple radiation patterns shown in Fig. 3.3 are generated due the varying level of mutual coupling between the elements in the array as the geometry is changed by activating the PIN diodes to change the length of the dipole. The RPDA has four states: *short-short*, *short-long*, *long-short*, and *long-long*. In the "*short*" and the "*long*" configuration, the switch on the antenna is inactive and active respectively. In contrast to the RCPA, the RPDAs display high correlation (Table 3.4) between the modes exited from different antenna elements but is still sufficient enough

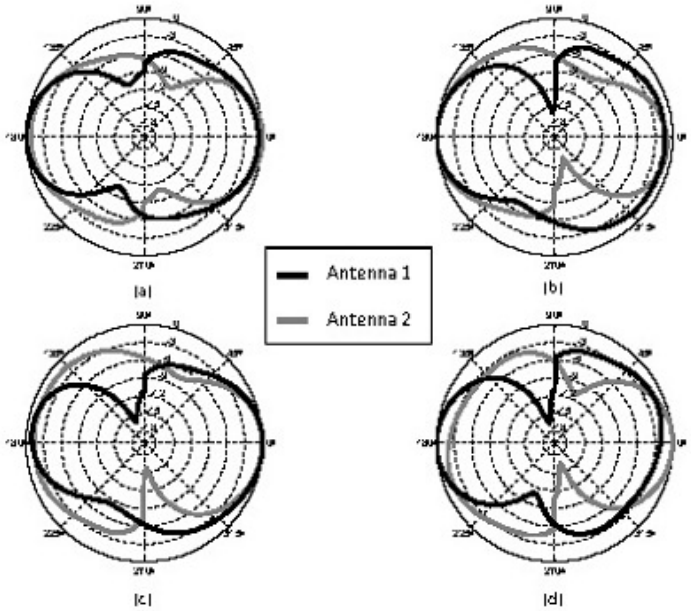

Figure 3.3: RPDA Radiation Patterns (in dB) in the azimuthal plane with antenna element separation of $\lambda/4$. a) *short-short*; b) *long-short*; c) *short-long*; d) *long-long* to generate uncorrelated channel samples. The relatively highly correlation exhibited by RCPA is compensated by the more number of patterns available for diversity and very high radiation efficiency, which provides sufficiently high SNR at the receiver.

Table 3.4: Spatial correlation between patterns generated at the same port of the RPDA

Short-short	*Long-short*	*Short-long*	*Long-long*
0.43	21	0.28	0.31

Table 3.5: Spatial correlation between patterns generated at the same port of the RPDA

	$E_{1,s-s}$	$E_{1,s-l}$	$E_{1,l-s}$	$E_{1,l-l}$
$E_{1,s-s}$	1	0.87	0.94	0.9
$E_{1,s-l}$	0.87	1	0.9	0.93
$E_{1,s-s}$	0.94	0.9	1	0.93
$E_{1,s-s}$	0.9	0.93	0.93	1

3.3 Measurement Setup

3.3.1 3 user 2×2 MIMO scenario

For analyzing the three user 2×2 MIMO network, we employ the set up reported in [22]. Channel measurements, we made use of HYDRA Software Defined Radio platform [24] in a 2×2 MIMO setup at 2.4 GHz band using 64 OFDM subcarriers, with 52 data subcarriers. The measurements were conducted on the third floor of the Bossone Research Center in Drexel University in an indoor setup. Three designated receiver nodes and three transmitter nodes were equipped with reconfigurable antenna, with each node equipped with two antenna elements. The network topology shown in Fig. 3.4 was then used to activate each transmitter-receiver pair to measure the channel response and then the superposition principle was used to recreate an

Table 3.6: Measured Radiation efficiency of the RCPA

	Antenna 1 (%)	*Antenna 2 (%)*
Short-short	84	75
Short-long	77	52
Long-short	48	77
Long-long	52	51

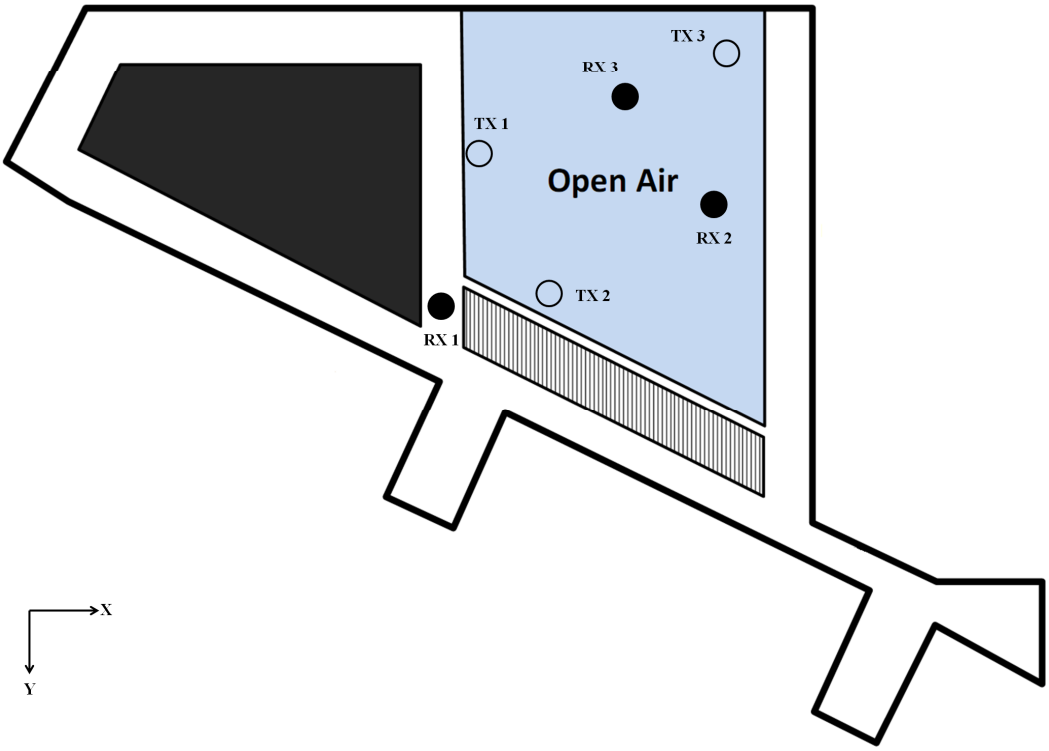

Figure 3.4: 3 User 2 × 2 MIMO Indoor Experimental Setup

interference-limited network. In order to further capture the small-scale fading effects, the receiver nodes were placed on a robotic antenna positioner and were moved to 40 different locations. Receiver 1 and 2 were moved $\frac{\lambda}{10}$ distance along y-axis and Receiver 3 was moved $\frac{\lambda}{10}$ distance along x-axis. For each position and each transmitter-receiver pair, 100 channel snapshots were captured and averaged for each subcarrier. After the completion of the measurement campaign, 240 channel samples were collected for each subcarrier and for each antenna configuration. This entire experiment was repeated for both RCPA and RPDA.

Chapter 4

Results and Discussion

In previous chapters we have studied how interference alignment can help increase sum capacity of interference networks and the experimental set up used to collect real world channel data for evaluating this enhancement. In this chapter we introduce the metrics used to study and benchmark the performance of interference alignment with reconfigurable antennas and subsequently quantify the obtained results. We start by providing an overview of the MIMO channel normalization procedure used to remove path loss and relative inefficiencies between antenna architectures. Using the normalized channel model, we then discuss the sum capacity formulation for multiuser networks using IA. Since, our central goal is to understand the impact of pattern diversity on sub-space orthogonality, we next introduce the measure of chordal dis-

tance between sub-spaces to quantify the amount of orthogonality achieved. Finally, we discuss the sum-rate scaling of IA and the gains achieved using reconfigurable antennas by defining the degrees of freedom of the interference network.

4.1 Performance Metrics and Evaluation

4.1.1 Normalization of Channel Values

We note that although, the normalized MIMO channel is not a standardized channel model, but nonetheless it is of considerable practical importance. Raw channel values collected through the field measurements using HYDRA and WARP are affected by real world propagation effects such as small scale fading and path loss, which are stochastic in nature. It is therefore imperative that we normalize all the channel values with a common factor before comparing the results from different antenna architectures or else stochastic channel effects could be mistaken for gain/loss in performance of the algorithm under consideration. The choice of the normalization factor often depends on the characteristic of the system being analyzed [25]. Since, our objective is to understand the performance improvements achieved using different reconfigurable antenna architectures, we choose to normalize out the effects of absolute path loss while conserving the relative difference of path loss between the receivers. Also, as observed in Sec. 3.2.1, different antenna architectures exhibit vari-

able efficiencies. Moreover, even within architecture under consideration, efficiency of different states varies. Therefore, we choose to normalize the effect of variable efficiency across the antenna architecture, while preserving the differences with the states. To achieve this, we proceed by forcing the most efficient states of both the antennas to receiver equal power. We then remove the effect of path loss to make sure that the capacity gains observed are solely because of the antenna characteristics [23]. Mathematically stated, this is achieved by normalizing the channels obtained from both the antennas separately with the normalization factor η, given as

$$\eta = \max_{i,j \in \Omega} \mathbb{E}\left[\sum_{f=1}^{F_s} \left\| \mathbf{H}^{[i,j]}(f) \right\|_F^2\right], \tag{4.1.1}$$

where the expectation was taken over all the 40 measurement locations. The normalized channels are then given by

$$\mathbf{H}_{normalized} = \mathbf{H}_{measured} \times \sqrt{\frac{NM \times F_s}{\eta}}. \tag{4.1.2}$$

where N represents the number of transmit antennas, M represents the number of receive antennas and F_s is the total number of subcarriers in the OFDM system. This type of normalization effectively equates the efficiency of the most efficient state of RCPA (Mode3) to the most efficient state of RPDA (short-short). Such an approach also preserves the frequency selective nature of the wireless channel, relative difference in efficiency between states of each antenna and topology of the network.

Here it's important to realize that the choice of the normalization factor is depended upon the characteristics of the system we wish to analyze. Alternate definitions for the factor are certainly possible but the results must then be carefully interpreted along similar lines. One such alternate factor is defined as

$$\eta_2 = \mathbb{E}\left[\sum_{f=1}^{F_s} \left\|\mathbf{H}^{[i,j]}(f)\right\|_F^2\right]. \tag{4.1.3}$$

The factor η_2 then should be defined individually for each state of the reconfigurable antenna. This removes all power variations across the states of the antenna and hence is invariant of relative power received. This enables a direct comparison of the eigenmodes of the channel which was not possible with our previous definition of the normalization factor.

4.1.2 Ergodic Sum Capacity

We begin our discussion of the capacity of multiuser, multi band interference channel with interference alignment precoding by defining the variables which will be used to present the capacity formulation and by motivating the capacity of single user, single band MIMO channel. The ergodic capacity of multi antenna gaussian channels was first studied by Telatar in [26]. Following the results presented there and assuming that our input symbol $\mathbf{x}$ is *circularly symmetric complex gaussian* and subject to a maximum power constraint of P i.e. $\mathbb{E}\left[\mathbf{x}^\dagger\mathbf{x}\right] \leq P$, the capacity of the single user

MIMO channel can be represented by

$$C = \max_{\mathbf{Q}: tr(\mathbf{Q})=P} \mathbb{E}\left[\log_2 \det(\mathbf{I}_M + \mathbf{HQH}^\dagger)\right], \tag{4.1.4}$$

where $\mathbf{Q}$ is the input covariance matrix of the symbol $\mathbf{x}$. The design of the optimal input covariance matrix depends on the channel state information (CSI) available at the receiver and transmitter. When perfect CSI is available at both the transmitter and receiver and the channel is slowly varying, the MIMO channel can be broken down into set of parallel SISO channels by performing *singular value decomposition* (SVD) i.e.

$$\mathbf{H} = \mathbf{UDV}^\dagger, \tag{4.1.5}$$

where the diagonal elements of $\mathbf{D}$ represent the strength of the eigenmodes of the channel and $\mathbf{U}$, $\mathbf{V}$ represent the left and right sigular vectors respectively. Optimum capacity can be then realized by waterfilling power across the eigenmodes of the channel [27] i.e.

$$\mathbf{Q} = \mathbf{VSV}^\dagger, \tag{4.1.6}$$

$$s_i = \left(\mu - \frac{1}{\sigma_i^2}\right), \tag{4.1.7}$$

where μ is the waterfill level, s_i is the power allocated to the ith eigenmode and σ_i^2 is the singular value associated with the ith eignmode. The ergodic channel capacity is

then given by

$$C_{perfect-CSI} = \mathbb{E}\left[\log_2 \det(\mathbf{I} + \mathbf{DSD}^\dagger)\right] \tag{4.1.8}$$

When no CSI is available at the transmitter, decomposition of the channel matrix is not possible and hence waterfilling across eigenmodes cannot be done. The best strategy in that scenario is too allocate equal power across all the modes. The capacity under this case is represented by

$$C_{No-CSI} = \mathbb{E}\left[\log_2 \det(\mathbf{I} + \frac{SNR}{N_t}\mathbf{HH}^\dagger)\right], \tag{4.1.9}$$

where it should be noted that the channel matrix represents normalized values.

In the single transmitter case discussed above, SNR is only affected by random noise added at the receiver. However, when multiple transmitters are present, the signal power received at every receiver is also affected by the interference power of unintended signals. Additionally, the transmission scheme, i.e. Multiple Access Channel (MAC) or Broadcast Channel (BC) , also affects the capacity formulation for the IC. Here, we are only concerned with the capacity of MIMO MAC channels. Let $\mathbf{R}_i$ represent the covariance matrix of this interference at the ith receiver, given by

$$\mathbf{R}_i = \sum_{\substack{j=1 \\ j\neq k}}^{K} \mathbf{H}^{[i,j]}\mathbf{Q}_j\mathbf{H}^{[i,j]\dagger} + \mathbf{I}. \tag{4.1.10}$$

Using this definition of $\mathbf{R}_i$ and (4.1.4), capacity of the link between the ith receiver, transmitter pair in a multiuser scenario can be represented by

$$C = \max_{\mathbf{Q}: tr(\mathbf{Q})=P} \mathbb{E}\left[\log_2 \det(\mathbf{I}_M + \mathbf{R}_i^{-1}\mathbf{H}^{[\mathbf{i},\mathbf{i}]}\mathbf{Q}\mathbf{H}^{[\mathbf{i},\mathbf{i}]\dagger})\right]. \tag{4.1.11}$$

Equation 4.1.11 represents the ergodic capacity of a single link, single band, in a multiuser network. We approximate the ergodic capacity by averaging the instantaneous capacity values over both space and time. The average sum-capacity of the multi band, multiuser network can then be approximated by [28],

$$C_{\Sigma-multiuser} = \frac{1}{F_s}\sum_{f=1}^{F_s}\sum_{k=1}^{K}\log_2 \det(\mathbf{I}_{d_k} + \mathbf{R}^{-1[k]}\mathbf{H}^{[k,k]}\mathbf{Q}^{[k]}\mathbf{H}^{[k,k]\dagger}), \tag{4.1.12}$$

As noted in Sec 2.2, IA precoders and decoders modify the effective channel matrix between the trasnmitter receiver pair, therefore, we modify the (4.1.12) to use the effective channel values, i.e.

$$C_{\Sigma-IA} = \frac{1}{F_s}\sum_{f=1}^{F_s}\sum_{k=1}^{K}\log_2 \det(\mathbf{I}_{d_k} + \mathbf{R}^{-1[k]}\mathbf{H}_{eff}^{[k,k]}\mathbf{Q}^{[k]}\mathbf{H}_{eff}^{[k,k]\dagger}), \tag{4.1.13}$$

where,

$$\mathbf{H}_{eff}^{[k,k]} = \mathbf{u}^{[k]}\mathbf{H}^{[k,k]}\mathbf{v}^{[k]\dagger}, \tag{4.1.14}$$

represents the effective channel between kth transmitter-receiver pair and

$$\mathbf{R}^{[k]} = \sigma^2\mathbf{u}^{[k]}\mathbf{u}^{[k]\dagger} + \sum_{\substack{j=1\\ j\neq k}}^{K}\mathbf{u}^{[k]}\mathbf{H}^{[k,j]}\mathbf{v}^{[j]}\mathbf{Q}^{[j]}\mathbf{v}^{[j]\dagger}\mathbf{H}^{[k,j]\dagger}\mathbf{u}^{[k]\dagger}, \tag{4.1.15}$$

represents the interference plus noise covariance matrix at the kth receiver.

4.1.3 Chordal Distance

As discussed in Sec. 3.1, interference alignment is only capacity optimal in the high SNR region. For low values of SNR, it suffers a performance degradation because of the signal component lost in the interference space after interference suppression at the receiver. Therefore, it is imperative to keep the signal and interference space roughly orthogonal, which would then minimize the projection of the signal lying in the interference space. This reduction in the signal power lost leads to performance improvement in terms of the sum-capacity achieved. To quantify this measure of orthogonality between the two sub spaces we use *chordal distance* (4.1.16), defined over the Grassmann manifold $\mathcal{G}(1,2)$ [29], as the distance metric:

$$d(\mathbf{X},\mathbf{Y}) = \sqrt{\frac{c_X + c_Y}{2} - \|O(\mathbf{X})^{\dagger} O(\mathbf{Y})\|_F^2}, \tag{4.1.16}$$

where c_X, c_Y denotes the number of columns in matrix $\mathbf{X}$,$\mathbf{Y}$ receptively and $O(\mathbf{X})$, $O(\mathbf{Y})$ denotes the orthonormal basis of $\mathbf{X}$, $\mathbf{Y}$. As represented in Fig. 4.1, the Grassmann manifold $\mathcal{G}(p,n)$, represents the collection of all the p dimensional linear sub-spaces embedded in n dimensions [30]. Each point on the Grassman manifold then represents a linear sub-space. Several different type of distance can be defined over these these linear subspaces [30], such as arc length, projection F-norm, projection 2-norm etc. Because of its simplicity we use the chordal 2-norm (chordal distance) distance to measure the orthogonality of subspaces in $\mathcal{G}(1,2)$ [29].

All the states of the reconfigurable antennas lead to varying channel realizations,

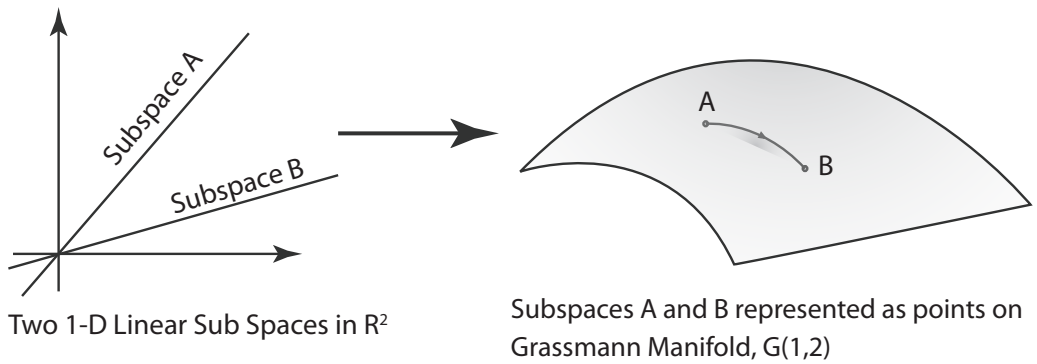

Figure 4.1: Conceptual representation of transformation from Euclidean space to Grassmann Manifold

which can be correlated or uncorrelated to each other affecting the chordal distance accordingly. The sum-rate performance (4.1.13) then becomes a function of the chordal distance between the two spaces. Motivated by [5], we define and use the total chordal distance across the 3 users as

$$\begin{aligned} D_{total} = d(\mathbf{H}^{[1,1]}\mathbf{v}^{[1]}, \mathbf{H}^{[1,2]}\mathbf{v}^{[2]}) + d(\mathbf{H}^{[2,2]}\mathbf{v}^{[2]}, \mathbf{H}^{[2,1]}\mathbf{v}^{[1]}) \\ + d(\mathbf{H}^{[3,3]}\mathbf{v}^{[3]}, \mathbf{H}^{[3,1]}\mathbf{v}^{[1]}). \end{aligned} \tag{4.1.17}$$

The metric in (4.1.17) is maximized when the signal and interference space are orthogonal at all the three receivers, which is desired for maximizing the sum capacity of the network. Therefore, a high chordal distance is empirically correlated to a higher sum-rate. Studying the behavior of D_{total} with and without using reconfigurable antennas, would then give us a better understanding of the impact of using pattern diversity at the physical layer.

4.1.4 Degrees of Freedom achieved

Consider a simple gaussian channel

$$Y = HX + N, \tag{4.1.18}$$

where the input symbol has a power budget, $\mathbb{E}\left[X^2\right] \leq P$ and $N \sim \mathcal{N}\left(0, \sigma^2\right)$. The capacity of this channel was calculated by Shannon and is equal to

$$C = \log_2\left(1 + P\frac{|H^2|}{\sigma^2}\right). \tag{4.1.19}$$

An approximation for this capacity expression can be obtained as follows

$$C \approx \log_2\left(P\right) + o\left(\log_2\left(P\right)\right). \tag{4.1.20}$$

The coefficient of the first term in the (4.1.20) is termed Degrees of Freedom (DoF) of the channel and represents the number of interference free signaling dimensions available for transmission. Since, currently it is not feasible to obtain exact capacity expressions for generalized interference channels, analyzing the obtaibed DoF can yield powerful insights into the behavior of the network. Using DoF, an approximate expression for a collection of such Gaussian channels can be expressed as

$$C \approx DoF \times \log_2\left(P\right) + o\left(\log_2\left(P\right)\right) \tag{4.1.21}$$

For the 3 user 2×2 MIMO channel, maximum of 3 DoF [4] are available, which translates to 3 simultaneous interference free streams. We study the achieved DoF

of IA with and without using reconfigurable antennas and compare the performance in Sec. 4.2. As asymptotically high SNR is not available in practical scenarios, an approximation for DoF (4.1.22) as defined in [4], is obtained by performing regression on the SNR v/s sum-rate curve.

$$DoF = \lim_{SNR \to \infty} \frac{C_{\Sigma}(SNR)}{\log_2(SNR)} \tag{4.1.22}$$

4.2 Results and Discussion

4.2.1 Closed form IA

We evaluate the performance impact of the reconfigurable antennas, by using the metrics discussed above and compare the performance of the two antenna architectures in this section. An SNR of 20 dB was maintained for all the nodes in the network which provided sufficient accuracy for the collection of channel samples and also allows us to extrapolate the performance in both high and low SNR ranges. The Cumulative Distribution Function, CDF, plots were generated using 240 data points collected from 40 different location of transmitter-receiver pair and 6 different topologies of the network. Each sample in the set of 240 points represents average capacity which has been calculated according to 4.1.13. We choose the most efficient operating states of RCPA and RPDA (*Mode 3* and *short-short* respectively) as the substitutes for comparison with non-reconfigurable antennas. This removes any loss in performance

due to antenna efficiency because our normalization procedure, Sec. 4.1.2, equates the most efficient modes of the the architectures to the same power level.

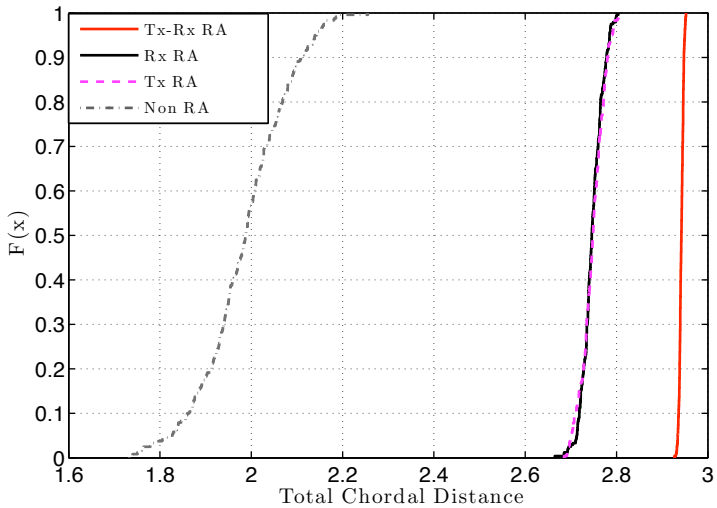

Figure 4.2: CDF of the total chordal distance achieved via RPDA

In Fig. 4.2 and Fig. 4.3, we show the CDF of the total chordal distance for RPDA and RCPA respectively. It can be observed that IA combined with reconfigurable antennas, significantly enhances the achieved chordal distance. We highlight that RPDA out performs RCPA in terms of percentage improvement, which can be attributed to the greater number of patterns available in RPDA, improving its pattern diversity. Also, the percentage improvement in chordal distance is almost the same for the two scenarios when RCPA is employed at both sides of the link (transmitter-receiver) and RPDA only at one side of the link (transmitter or receiver). This equal improvement is observed because of the equal number of reconfigurable states available in the net-

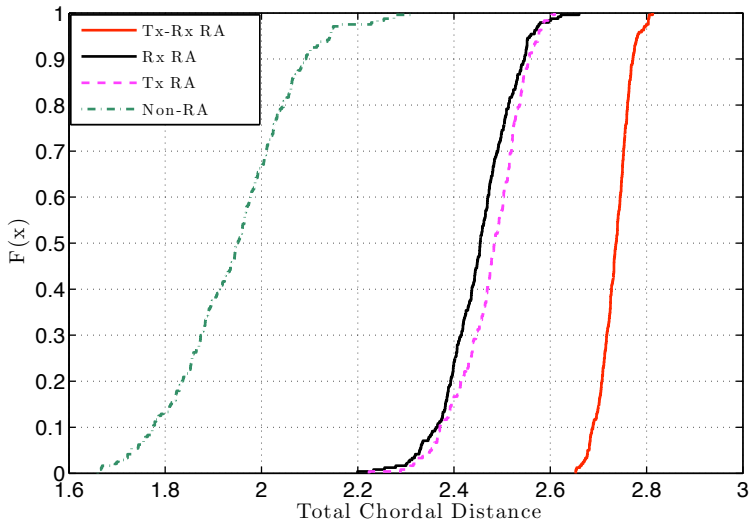

Figure 4.3: CDF of the total chordal distance achieved via RCPA

work for optimal mode selection in both the cases. Summarized results in Table 4.1 indicate that the subspaces designed via optimal selection of the antenna state can achieve close to perfect orthogonality and total chordal distance can approach the theoretical maximum value of 3.

Further, in Fig. 4.4 and 4.5 we study the impact of enhanced chordal distance on the sum capacity performance of IA. Although, we observe that adding reconfigurability enhances the sum rate performance of IA, the gains achieved are less prominent for RCPA despite the enhanced chordal distance seen in Table 4.1. This apparent independence of sum-rate and chordal distance performance is observed because chordal distance only exploits the underlying orthonormal space to measure distance, making it insensitive to the relative difference in the efficiency of states of

Table 4.1: Mean value of total chordal distance

	RCPA	% Increase over Non-RA	RPDA	% Increase over Non-RA
IA Non-RA	1.94	N/A	1.99	N/A
IA Tx-RX RA	2.73	40.72	2.94	47.74
IA RX RA	2.38	27.84	2.75	38.19
IA TX RA	2.45	26.29	2.75	38.19

the reconfigurable antennas. Since the states of RPDA have efficiency close to each other, its sum rate performance is better than RCPA. It can be observed that, for both RPDA and RCPA, the performance of transmitter and receiver side configuration are similar since the chordal distances obtained are also quite similar. Similar performance in terms of sum-rate shows that given equal efficiency, chordal distance is closely related to sum rate performance.

We observe performance gains of the order of 45 % and 15 % (at 20 dB SNR) over non-reconfigurable antennas respectively with RPDA and RCPA employed at both transmitter and receiver. We also compare IA to other transmit strategies such as TDMA, networks using no interference avoidance strategy (Ad hoc) with and without reconfigurable antennas and observe that as predicted in theory, IA outperforms them all.

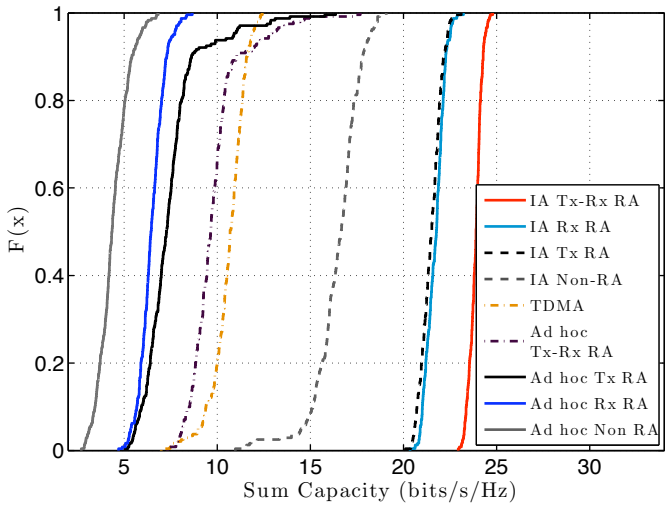

Figure 4.4: Empirical CDF plot of Sum - Capacity for RPDA (SNR = 20 dB)

In Fig. 4.6 and 4.7, we show the sum capacity in different SNR regimes. The plots illustrate that IA achieves maximum sum capacity with full reconfigurability at both transmitter and receiver. The marginal gains realized because of increased chordal distance are more prominent in the low SNR region since non-orthogonal spaces degrade the performance of IA in that regime [6] [7]. As more reconfigurable states are added to the network, increasing gains in sum capacity are observed. Characterizing DoF from the slopes of the traces in Fig. 4.6 and 4.7 reveals that using IA with reconfigurable antennas can improve the achieved DoF while increasing the sum rate at the same time. The achieved DoF are summarized in Table 4.3. For the three user 2×2 MIMO system, a maximum of 3 DoF can be achieved. With RPDA at both transmitter and receiver we were able to achieve close to 2.94 as compared to

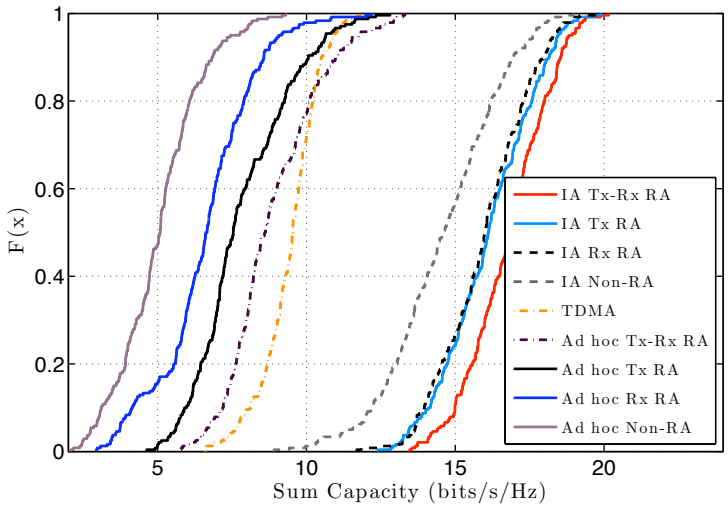

Figure 4.5: Empirical CDF plot of Sum - Capacity for RCPA (SNR = 20 dB)

2.74 with non-reconfigurable structures. Additionally, it can be seen that TDMA achieved only a max of 1.74 as compared to 2.94 achieved by IA. Therefore, our measurements also show that IA performs better than TDMA under realistic channels and its performance can further be enhanced using reconfigurable antennas [31].

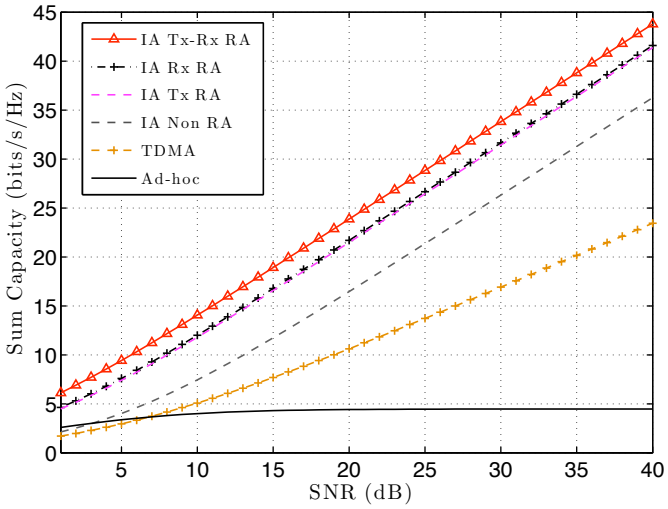

Figure 4.6: Sum-Rate v/s SNR for RPDA

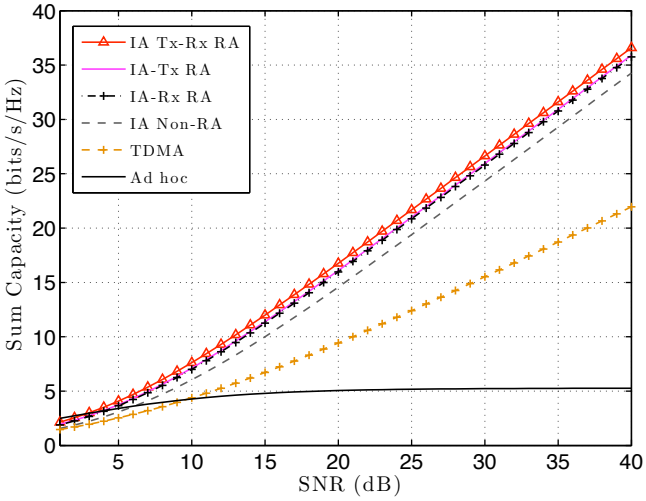

Figure 4.7: Sum-Rate v/s SNR for RCPA

Table 4.2: Comparison of mean value of sum capacity achieved

Configuration	RPDA	% Increase over Non-RA	RCPA	% Increase over Non-RA
Tx Rx-RA	23.9	45	16.76	15.1
Rx RA	21.7	31.8	16.1	10.5
Tx RA	21.29	30.51	15.96	9.52
Non -RA	16.46	N/A	14.57	N/A

Table 4.3: Degrees of Freedom (DoF) achieved

	RCPA	RPDA
TDMA	1.64	1.74
IA Non-RA	2.65	2.74
IA Tx-Rx-RA	2.77	2.95
TX Rx-RA	2.74	2.90
TX Tx-RA	2.73	2.90

Chapter 5

Conclusion and Future Work

In this work, we have shown that reconfigurable antennas can significantly enhance the performance of IA by enabling an additional degree of freedom in terms of channel states available, for optimal state selection. We quantified the effect of pattern diversity on enhanced chordal distance and on the sum-capacity performance of the network. The results presented empirically prove that sum-capacity is directly proportional to chordal distance between the signal and interference space. Further it was shown that marginal gains achieved using reconfigurable antennas are more prominent in the low SNR region. Along with the enhanced sum-capacity achieved, we also showed that DoF of the interference channel achieved via reconfigurable antennas are higher from a non-reconfigurable system. These results from measured channel data prove the feasibility of using reconfigurable antennas for enhancing interference

management techniques such as IA.

5.1 Future Work

The results presented in this work show that reconfigurable antennas can play an important role in scaling the sum-capacity of networks using IA as the interference management scheme. However, we note that for enabling real-time implementation of such a system we need to address several open problems. We outline some of the issues below, which are shaping our future work in this domain.

- **Optimum State Selection**: Physical propagation environment is the single most important resource in wireless communications. Reconfigurable antennas help us realize multiple of these propagation environments, which we then exploit for increasing system capacity. In order to realize this gain, it is imperative that we choose a state, which gives us the best propagation path. This task is not trivial since the performance of states cannot be predicted before real operation. As the number of states available increase, the search space for optimization increases exponentially in a network setting, making the process of optimization even more complex. In this work we analyzed the raw channel data collected in an offline fashion and employed chordal distance as the criterion to select the optimal state. We note that this scheme is not real time and involves optimization over all the combinations of states available thereby incurring lot

of overhead.

Recently, the authors in [32], proposed a machine learning algorithm based on the multi-arm bandit selection framework, for optimal state selection, which drastically reduces the search space as well as the signaling overhead required. Exploring the possibility of designing such online learning techniques, which reduce the search space and optimize a cost function based on IA is therefore of practical interest.

- **Real World Feasibility Analysis of BIA**: IA comes at the expense of exchanging instantaneous global channel knowledge at all the transmitter-receiver pairs, a requirement that is seldom satisfied in real world networks. To overcome this requirement, blind alignment schemes have been proposed that only consider switching patterns of reconfigurable antennas at the receivers. However, unlike iterative IA algorithms that have been independently validated through many experimental studies [7], [6], performance of BIA is still to be fully understood. We outline some of the real world effects that need to be better understood before BIA can be implemented in real systems.

  - BIA algorithms rely on synchronized frame reception for alignment. In [33], it was shown that BIA fails completely with synchronization mismatch of one OFDM symbol. It would therefore be interesting to observe and quantify how the algorithms would perform in more realistic scenarios,

i.e. when overheads of higher layers such as MAC are also included and synchronized reception is not guaranteed. Future work in this direction should also consider design of more robust algorithms that are not sensitive to synchronization.

- Current BIA algorithms assume a large channel coherence time since they rely on obtaining channels that remain static over the duration of a sypersymbol and only change with states of reconfigurable antenna [1]. This assumption leads to lot of interference leakage from one alignment block to the other. Since, this assumption of large coherence time is difficult to satisfy in real channels, it is important to study how the system performance degrades with decreasing coherence time. Emphasis should be on algorithms, which are independent of this assumption and hence more robust.

- As outlined in [1], the structure of the sypersymbol and the corresponding alignment blocks depends on the network architecture, number of transmitter receiver pairs and the number of antennas with which they are equipped. As the number of users and antennas increases, the alignment algorithm becomes highly convoluted with supersymbols of very long durations. With supersymbols lasting for several time slots, synchronization and coherence requirements become even more stringent coupled with the

need of more frequent switching of the antenna states. How fast the reconfigurable antennas can switch their states and how stable are the corresponding states, will then present a bottleneck in scaling the capacity of BIA systems and therefore constitutes an important future direction.

- **State selection for BIA**: The problem of optimal reconfigurable state selection presents different set of challenge in BIA than the ones discussed above. In IA our emphasis was on reducing the search space for selection and reducing the signaling overheard required for exchanging the corresponding CSIT. In context of BIA, the challenge is to select the modes that help in minimizing interference leakage, which results from low coherence time. The algorithms presented in [1] neglect the fact that modern reconfigurable antennas are equipped with more number of states than required by the alignment algorithm. How do we than select a subset of modes form the available set can greatly improve or degrade the performance of alignment algorithm. Therefore, an algorithm that selects the optimum subset of modes will form a critical element of our future work.

References

[1] T. Gou, C. Wang, and S. Jafar, "Aiming perfectly in the dark-blind interference alignment through staggered antenna switching," in *GLOBECOM 2010, 2010 IEEE Global Telecommunications Conference*. IEEE, 2010, pp. 1–5.

[2] D. Tse, "Its easier to approximate," in *Plenary talk, IEEE International Symposium on Information Theory (ISIT), Seoul, Korea*, 2009.

[3] H. Sato, "The capacity of the gaussian interference channel under strong interference (corresp.)," *Information Theory, IEEE Transactions on*, vol. 27, no. 6, pp. 786–788, 1981.

[4] V. Cadambe and S. Jafar, "Interference alignment and degrees of freedom of the-user interference channel," *Information Theory, IEEE Transactions on*, vol. 54, no. 8, pp. 3425–3441, 2008.

[5] H. Sung, S. Park, K. Lee, and I. Lee, "Linear precoder designs for K-user interference channels," *Wireless Communications, IEEE Transactions on*, vol. 9,

no. 1, pp. 291–301, 2010.

[6] O. El Ayach, S. Peters, and R. Heath, "The feasibility of interference alignment over measured MIMO-OFDM channels," *Vehicular Technology, IEEE Transactions on*, vol. 59, no. 9, pp. 4309–4321, 2010.

[7] O. González, D. Ramirez, I. Santamaria, J. Garcia-Naya, and L. Castedo, "Experimental validation of interference alignment techniques using a multiuser MIMO testbed," in *Smart Antennas (WSA), 2011 International ITG Workshop on*. IEEE, 2011, pp. 1–8.

[8] J. Boerman and J. Bernhard, "Performance study of pattern reconfigurable antennas in MIMO communication systems," *Antennas and Propagation, IEEE Transactions on*, vol. 56, no. 1, pp. 231–236, 2008.

[9] B. Cetiner, H. Jafarkhani, J. Qian, H. Yoo, A. Grau, and F. De Flaviis, "Multifunctional reconfigurable MEMS integrated antennas for adaptive MIMO systems," *Communications Magazine, IEEE*, vol. 42, no. 12, pp. 62–70, 2004.

[10] A. Sayeed and V. Raghavan, "Maximizing MIMO capacity in sparse multipath with reconfigurable antenna arrays," *Selected Topics in Signal Processing, IEEE Journal of*, vol. 1, no. 1, pp. 156–166, 2007.

[11] S. Jafar, *Interference Alignment-A New Look at Signal Dimensions in a Communication Network*, 2011.

[12] M. Razaviyayn, M. Sanjabi Boroujeni, and Z. Luo, "Linear transceiver design for interference alignment: Complexity and computation," in *Signal Processing Advances in Wireless Communications (SPAWC), 2010 IEEE Eleventh International Workshop on*. IEEE, 2010, pp. 1–5.

[13] C. Yetis, T. Gou, S. Jafar, and A. Kayran, "On feasibility of interference alignment in MIMO interference networks," *Signal Processing, IEEE Transactions on*, vol. 58, no. 9, pp. 4771–4782, 2010.

[14] S. Jafar, "Blind interference alignment," *Selected Topics in Signal Processing, IEEE Journal of*, no. 99, pp. 1–1, 2011.

[15] ——, "Exploiting channel correlations-simple interference alignment schemes with no CSIT," in *GLOBECOM 2010, 2010 IEEE Global Telecommunications Conference*. IEEE, 2010, pp. 1–5.

[16] J. Bernhard, "Reconfigurable antennas," *Synthesis Lectures on Antennas*, vol. 2, no. 1, pp. 1–66, 2007.

[17] A. Grau, H. Jafarkhani, and F. De Flaviis, "A reconfigurable multiple-input multiple-output communication system," *Wireless Communications, IEEE Transactions on*, vol. 7, no. 5, pp. 1719–1733, 2008.

[18] H. Pan, G. Huff, T. Roach, Y. Palaskas, S. Pellerano, P. Seddighrad, V. Nair, D. Choudhury, B. Bangerter, and J. Bernhard, "Increasing channel capacity

on MIMO system employing adaptive pattern/polarization reconfigurable antenna," in *Antennas and Propagation Society International Symposium, 2007 IEEE*. IEEE, 2007, pp. 481–484.

[19] D. Piazza, M. D'Amico, and K. Dandekar, "Performance improvement of a wideband MIMO system by using two-port RLWA," *Antennas and Wireless Propagation Letters, IEEE*, vol. 8, pp. 830–834, 2009.

[20] D. Piazza, N. Kirsch, A. Forenza, R. Heath, and K. Dandekar, "Design and evaluation of a reconfigurable antenna array for MIMO systems," *Antennas and Propagation, IEEE Transactions on*, vol. 56, no. 3, pp. 869–881, 2008.

[21] A. Forenza and R. Heath Jr, "Benefit of pattern diversity via two-element array of circular patch antennas in indoor clustered MIMO channels," *Communications, IEEE Transactions on*, vol. 54, no. 5, pp. 943–954, 2006.

[22] D. Piazza, P. Mookiah, M. D'Amico, and K. Dandekar, "Experimental analysis of pattern and polarization reconfigurable circular patch antennas for MIMO systems," *Vehicular Technology, IEEE Transactions on*, vol. 59, no. 5, pp. 2352–2362, 2010.

[23] J. Kountouriotis, D. Piazza, P. Mookiah, M. DAmico, and K. Dandekar, "Reconfigurable antennas and configuration selection methods for MIMO ad hoc

networks," *EURASIP Journal on Wireless Communications and Networking*, vol. 2011, no. 1, pp. 1–14, 2011.

[24] K. Mandke, S. Choi, G. Kim, R. Grant, R. Daniels, W. Kim, R. Heath, and S. Nettles, "Early results on HYDRA: A flexible mac/phy multihop testbed," in *Vehicular Technology Conference, 2007. VTC2007-Spring. IEEE 65th.* IEEE, 2007, pp. 1896–1900.

[25] S. Loyka and G. Levin, "On physically-based normalization of MIMO channel matrices," *Wireless Communications, IEEE Transactions on*, vol. 8, no. 3, pp. 1107–1112, 2009.

[26] E. Telatar, "Capacity of multi-antenna gaussian channels," *European transactions on telecommunications*, vol. 10, no. 6, pp. 585–595, 1999.

[27] A. Goldsmith, S. Jafar, N. Jindal, and S. Vishwanath, "Capacity limits of MIMO channels," *Selected Areas in Communications, IEEE Journal on*, vol. 21, no. 5, pp. 684–702, 2003.

[28] R. Blum, "MIMO capacity with interference," *Selected Areas in Communications, IEEE Journal on*, vol. 21, no. 5, pp. 793–801, 2003.

[29] D. Love and R. Heath, "Limited feedback unitary precoding for spatial multiplexing systems," *Information Theory, IEEE Transactions on*, vol. 51, no. 8, pp. 2967–2976, 2005.

[30] A. Edelman, T. Arias, and S. Smith, "The geometry of algorithms with orthogonality constraints," *Arxiv preprint physics/9806030*, 1998.

[31] A. Tsai, J. Huang, L. Wang, and R. Hwang, "Capacity comparison for CSG and OSG OFDMA femtocells," in *GLOBECOM Workshops (GC Wkshps), 2010 IEEE*. IEEE, 2010, pp. 653–658.

[32] N. Gulati, D. Gonzalez, and K. Dandekar, "Learning algorithm for reconfigurable antenna state selection," in *IEEE Radio and Wireless Symposium*. IEEE, 2012.

[33] K. Miller, A. Sanne, K. Srinivasan, and S. Vishwanath, "Enabling real-time interference alignment: promises and challenges," in *Proceedings of the thirteenth ACM international symposium on Mobile Ad Hoc Networking and Computing*. ACM, 2012, pp. 55–64.